East European Journal of Physics. 3. 659-664 (2026)
DOI:10.26565/2312-4334-2026-3-62 ISSN 2312-4334

QUANTITATIVE TRANSMISSION ELECTRON MICROSCOPY ANALYSIS OF AMYLOID FIBRIL MORPHOLOGY

V. Trusova[1]*, U. Malovytsia[1], O. Zhytniakivska[1], K. Chkuaseli[1], S. Bogatyrenko[2], G. Gorbenko[1]
[1]Department of Medical Physics and Biomedical Nanotechnologies, V.N. Karazin Kharkiv National University
4 Svobody Sq., Kharkiv, 61022, Ukraine
[2]Department of Materials for Reactor Building and Physical Technologies, V.N. Karazin Kharkiv National University
4 Svobody Sq., Kharkiv, 61022, Ukraine
**Corresponding Author email: valerija.trusova@karazin.ua*
Received May 5, 2026; revised July 29, 2026; accepted August 12, 2026

Amyloid fibrils are increasingly regarded as versatile protein-based nanomaterials whose functional properties depend not only on their molecular cross-β architecture but also on their supramolecular morphology. The present study was undertaken to compare the mesoscale organization of albumin, insulin, and lysozyme fibrillar assemblies using quantitative transmission electron microscopy. Representative TEM images were analyzed by a standardized image-processing workflow based on segmentation, skeletonization, orientation analysis, and connected-object morphometry. The resulting descriptors included projected fibril/aggregate area fraction, skeleton length density, apparent junction/crossover and endpoint densities, local width, object density, Feret length, aspect ratio, and orientation anisotropy. Insulin displayed the highest projected area fraction, skeleton length density, object density, endpoint density, and apparent junction/crossover density, indicating a compact and highly fragmented architecture dominated by numerous short rod-like elements. In contrast, lysozyme fibrils exhibited the greatest median Feret length and aspect ratio, consistent with a stronger contribution of longitudinal elongation and the formation of more anisometric structures. Albumin showed an intermediate morphology characterized by comparatively sparse, curvilinear fibrils and lower densities of discrete objects and endpoints. Orientation distributions were broad for all three systems, and the corresponding anisotropy indices remained low, demonstrating predominantly isotropic rather than globally aligned organization. These findings indicate that the three protein systems occupy distinct regimes of amyloid assembly, ranging from fragmentation-dominated architectures to more elongated fibrillar networks. The quantitative framework established here provides a basis for relating amyloid morphology to surface accessibility, connectivity, mechanical behavior, and the design of fibril-based hydrogels, biosensors, drug-delivery platforms, and nanocomposites.
Keywords: *Amyloid fibrils; Transmission electron microscopy; Quantitative image analysis; Fibril morphology; Supramolecular organization; Skeletonization; Orientation anisotropy; Protein nanomaterial*

Amyloid fibrils constitute a broad class of highly ordered protein assemblies characterized by a conserved cross-β structural motif [1,2]. Despite this common molecular architecture, their supramolecular morphology can vary substantially depending on protein sequence, solution conditions, aggregation pathway, fibril maturation, and sample preparation [3,4]. Accordingly, amyloid assemblies may form long isolated filaments, short rod-like fragments, laterally associated bundles, dense interconnected networks, or heterogeneous mixtures containing both fibrillar and non-fibrillar material. This mesoscale organization is functionally relevant because fibril dimensions, fragmentation, bundling, packing density, and network connectivity can influence gel formation, mechanical behavior, colloidal stability, molecular accessibility, and interactions with other biomolecular or nanoscale components [5].

Transmission electron microscopy (TEM) is among the most widely used techniques for direct visualization of amyloid fibrils because it enables assessment of their morphology at nanometer-scale resolution [6,7]. However, TEM-based assessment of amyloid morphology often remains predominantly descriptive, which limits the objectivity, reproducibility, and cross-sample comparability of structural interpretations. This limitation becomes particularly relevant when protein systems differ simultaneously in fibril abundance, contour organization, degree of overlap, and local connectivity. Quantitative image analysis is therefore essential for translating visually apparent morphological differences into reproducible and biologically interpretable structural descriptors. The need for such analysis becomes especially evident when fibrillar systems display fundamentally different modes of organization [8]. A relatively sparse population of elongated filaments cannot be compared meaningfully with a dense field of short overlapping rods using a single descriptor alone. Likewise, parameters derived from isolated fibrils may not adequately represent highly entangled or locally bundled networks. A comprehensive comparison should therefore consider several complementary features of the fibrillar architecture, including projected material coverage, fibrillar density, degree of fragmentation, apparent connectivity, directional organization, and object elongation.

In the present work, the morphology of albumin (BSAF), insulin (InsF), and lysozyme (LzF) fibrillar assemblies was examined comparatively using quantitative analysis of representative TEM images. These three systems were selected because they exhibit markedly different supramolecular organizations, ranging from relatively sparse elongated fibrils to dense populations of short fragments and extended network-like structures. The study aimed to identify and

Cite as: V. Trusova, U. Malovytsia, O. Zhytniakivska, K. Chkuaseli, S. Bogatyrenko, G. Gorbenko, East Eur. J. Phys. 3, 659 (2026), https://doi.org/10.26565/2312-4334-2026-3-62

quantify the principal morphological distinctions between the protein assemblies and to establish a coherent framework for interpreting their projected density, structural organization, connectivity, orientation, and characteristic dimensions. By integrating complementary image-derived parameters, the analysis provides a more objective description of fibril morphology than qualitative inspection alone and highlights the distinct modes of supramolecular organization adopted by the three protein systems.

METHODS

Amyloid fibrils of human insulin, chicken hen egg white lysozyme and bovine serum albumin were prepared by dissolving 10 mg of corresponding protein in 10 ml of glycine buffer, pH 2.0, followed by incubation at 60 °C for 14 days [9]. Fibril formation was confirmed by transmission electron microscopy. For sample preparation, a 10 μL aliquot of each fibril suspension was applied to a carbon-coated TEM grid and allowed to adsorb for 1 min, after which excess liquid was removed by blotting. The grids were subsequently negatively stained with 10 μL of 1.5% (w/v) phosphotungstic acid for 30 s, blotted, rinsed three times with deionized water, and air-dried. Electron micrographs were acquired using an EM-125 transmission electron microscope (Selmi, Ukraine). Representative micrographs were selected for comparative morphometric analysis in Fiji [10]. Each image was cropped to exclude scale bars, labels, montage borders, and other non-biological elements. The analyzed images had identical dimensions of 1382×876 pixels and were calibrated using a spatial resolution of 0.8 nm per pixel. Accordingly, each field represented an area of approximately 0.775 μm^2, allowing direct comparison of area-normalized descriptors among the three protein systems. Quantitative image analysis was performed using a standardized digital morphometry workflow designed to characterize the projected organization of fibrillar assemblies at the field level. The same preprocessing and segmentation procedure was applied to all images to minimize operator-dependent variability. The analyzed parameters and their description are given in Table 1.

Table 1. Quantitative descriptors used for comparative TEM morphometry

Parameter	Operational definition	Morphological significance
Projected fibril/aggregate area fraction, %	Percentage of pixels within the analyzed field assigned to fibrillar or aggregate material	Describes the proportion of the projected TEM field occupied by protein assemblies
Projected skeleton length density, μm^{-1}	Total length of the skeletonized fibrillar network normalized to the analyzed field area	Reflects the amount of projected fibrillar backbone per unit area
Apparent junction/crossover density, μm^{-2}	Number of skeleton junctions normalized to the analyzed field area	Describes the apparent connectivity or frequency of projected fibril intersections
Endpoint density, μm^{-2}	Number of skeleton endpoints normalized to the analyzed field area	Provides an indicator of fragmentation and object discontinuity
Orientation anisotropy index	Axial concentration of fibril orientations on a scale from 0 to 1	Values close to 0 indicate an isotropic or randomly oriented field, whereas values approaching 1 indicate strong preferential alignment
Orientation dispersion, °	Angular spread of the fibril-orientation distribution	Indicates a distribution of orientations
Mask-derived local width, nm	Local thickness of the segmented structure estimated from the binary mask around the skeleton centerline	Provides a comparative measure of apparent projected thickness
Connected-object density, μm^{-2}	Number of spatially separated threshold-positive objects normalized to the field area	Reflects the abundance of individually segmented structures
Feret length, nm	Maximum caliper distance across a connected segmented object	Represents the maximum projected dimension of an object and provides an approximate measure of fragment or rod length.
Aspect ratio	Ratio of the major projected object dimension to its minor dimension	Describes the fibril elongation

RESULTS AND DISCUSSION

As seen in Fig. 1, all three proteins are characterized by distinct modes of supramolecular organization despite the common cross-β character of amyloid fibrils. Specifically, BSAF formed an open population of long, curved fibrils separated by large fibril-poor regions. InsF, in turn, produced a markedly denser field dominated by numerous short rod-like elements, whereas LzF formed fewer, more extended fibrillar objects with occasional crossings and local bundling. These morphologies reflect different physical states of fibrillar matter rather than simple differences in fibril abundance. Amyloid polymorphism extends from the molecular packing of protofilaments to their mesoscale length, curvature, lateral association, and spatial organization, all of which are shaped by the balance among nucleation, elongation, fragmentation, and fibril-fibril interactions [11,12].

The conservative segmentation and skeletonization outputs are shown in Fig. 2. These images were used primarily to confirm that the quantified signal followed the visible fibrillar contours rather than broad staining gradients. The

numerical values therefore represent projected descriptors of the selected TEM fields, not bulk fibril concentration or three-dimensional network structure.

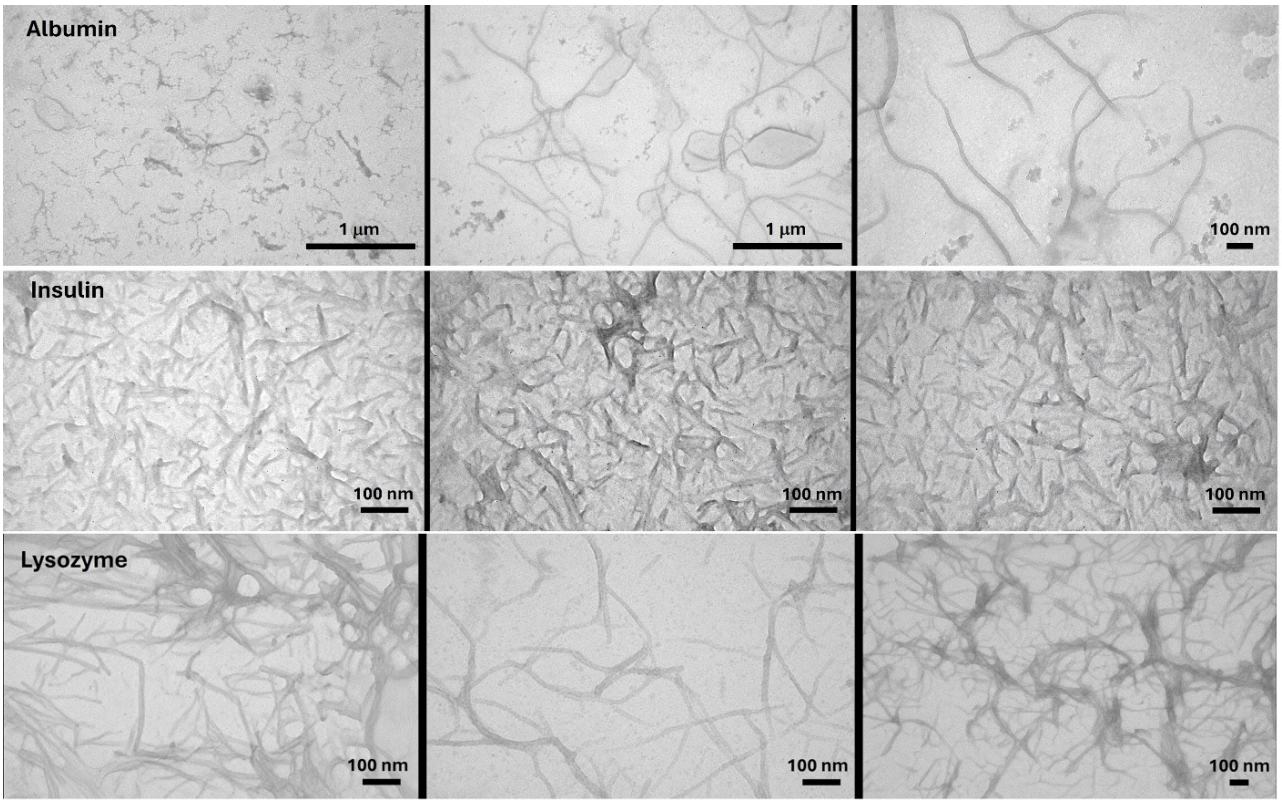

Figure 1. TEM images of albumin, insulin and lysozyme amyloid fibrils

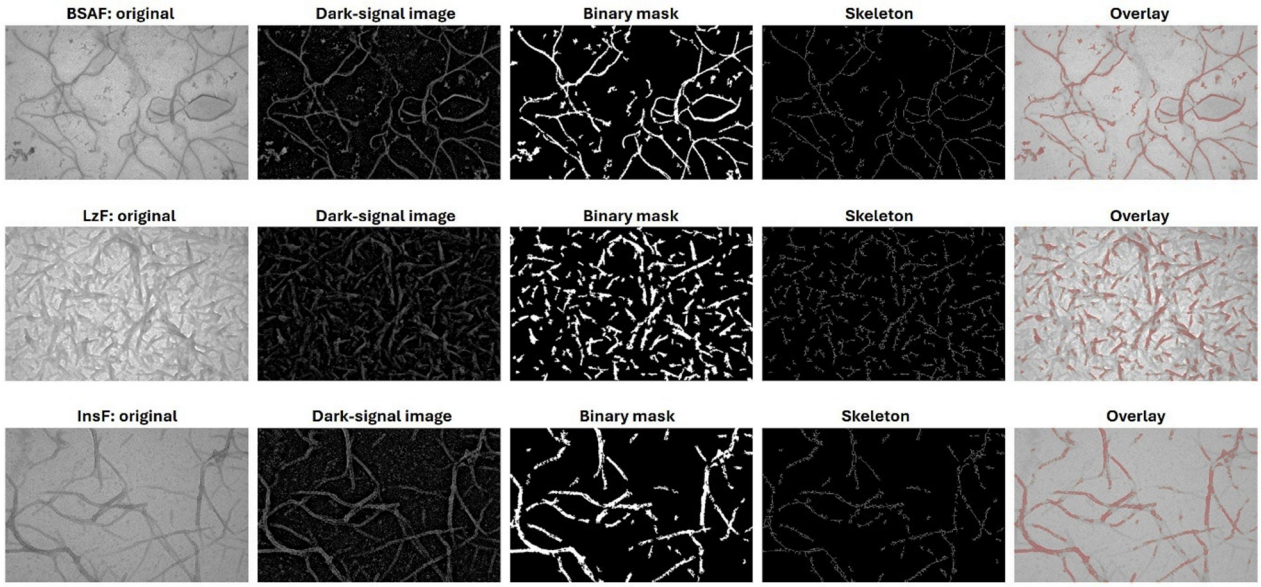

Figure 2. Quality-control representation of the image-analysis workflow. Original TEM images, extracted fibril-associated signal, binary masks, skeletons, and overlays are shown for each protein. The analysis retained the principal fibrillar structures while limiting inclusion of the heterogeneous TEM background

The quantitative parameters derived from image analysis are summarized in Table 2. Evaluation of these parameters revealed that InsF represents the most crowded and fragmentation-rich system. It showed the highest projected area fraction (14.58%), skeleton length density (30.98 μm^{-1}), connected-object density (232.32 μm^{-2}), endpoint density (2358.01 μm^{-2}), and apparent junction/crossover density (1600.40 μm^{-2}). Relatively high values of these quantities indicate that the dense insulin network is generated predominantly by a large number of short fibrillar units rather than by a few massive aggregates.

From mechanical perspective, the observed pattern of InsF is compatible with an assembly regime in which longitudinal growth is counterbalanced by breakage, repeated nucleation, or limited fibril maturation. Though TEM cannot distinguish among these pathways, it clearly demonstrates, however, a high-end-density population. Such a state can be biologically relevant because fibril ends and newly generated surfaces influence seeding, monomer recruitment, membrane contact, and cellular handling. Shortening of amyloid fibrils has been associated with enhanced particle number and altered cytotoxicity in other systems [13], although toxicity cannot be inferred from morphology alone.

Table 2. Quantitative morphometric parameters of amyloid fibrils obtained from TEM images

Metric	BSAF	InsF	LzF
Projected fibril/aggregate area fraction, %	10.41	14.58	9.85
Skeleton length density, μm^{-1}	21.09	30.98	19.34
Apparent junction/crossover density, μm^{-2}	929.27	1600.40	984.76
Endpoint density, μm^{-2}	1201.59	2358.01	1259.67
Connected-object density, μm^{-2}	101.96	232.32	80.02
Orientation anisotropy index	0.0027	0.0653	0.0634
Mean mask-derived local width, nm	5.77	5.06	5.77
Mean Feret length, nm	43.54	44.32	48.84
Mean aspect ratio	2.36	2.66	3.15

The same architecture may also be advantageous in engineered amyloid materials. A large number of short fibrillar objects provide abundant accessible surface and terminal sites for molecular adsorption or functionalization. Conversely, the limited contour length of individual rods may reduce their capacity to bridge large distances unless the particle concentration is sufficiently high to produce frequent contacts. The elevated junction density observed for InsF suggests that this requirement is met within the deposited layer, making the system potentially suitable for dense composite phases or highly populated interfacial coatings rather than sparse load-bearing networks.

In turn, LzF displayed the opposite tendency. Its projected coverage and object density were lower, yet the median Feret length (48.84 nm) and aspect ratio (3.15) were the highest among the three proteins under study. This combination indicates an elongation-dominated organization in which fewer fibrils extend over larger distances. Lysozyme is known to form extended amyloid fibrils under acidic conditions and to propagate through seeded growth, while protofibril association may also contribute to fibril development [14]. In physical terms, increased aspect ratio improves the ability of a fibril to connect spatially separated regions and lowers the concentration required for entanglement or network spanning. Accordingly, the lysozyme morphology is more compatible with reinforcement, bridging, and scaffold formation than the highly fragmented insulin architecture, although direct rheological or mechanical measurements would be required to test this prediction.

Fig. 3 illustrates the orientation plots which describe how frequently fibrillar segments are aligned at each angle within the image plane. A narrow histogram with a pronounced peak would indicate that a large fraction of fibrils shares a common preferred direction, whereas a broad or nearly uniform distribution reflects a predominantly isotropic arrangement with no dominant macroscopic alignment. The anisotropy index provides a complementary scalar measure of the same behavior: values approaching 0 correspond to random orientation, while values approaching 1 indicate strong directional ordering. As seen from this figure, all proteins exhibited broad orientation distributions. Furthermore, BSAF showed anisotropy index close to zero, whereas insulin and lysozyme displayed only slightly higher values, both below 0.07. These results indicate that none of the fibrillar populations formed a globally aligned architecture within the analyzed fields. Instead, the fibrils were distributed over many directions, consistent with isotropic deposition and local network formation. Although individual fibrils or bundles may exhibit locally coherent orientation, such local alignment does not translate into long-range orientational order at the scale of the full TEM field. In the present context, it should be noted that macroscopic alignment of amyloid fibrils emerges only when orientational interactions between elongated objects are sufficiently strong, typically at high effective concentration and aspect ratio or under external fields, flow, confinement, or surface-mediated ordering. In the absence of these conditions, fibrils may remain globally isotropic even when individual filaments are rigid and highly elongated. The broad histograms observed here, therefore suggest that the dominant differences among the three systems arise primarily from fibril abundance, fragmentation, elongation, and connectivity rather than from nematic-like ordering. This orientational isotropy also has functional implications. Accordingly, isotropic fibrillar networks are expected to exhibit more direction-independent mechanical and transport properties, whereas highly aligned assemblies may display anisotropic stiffness, diffusion, and molecular accessibility. Thus, the weak global orientation observed in all three samples indicates that their projected architectures are unlikely to impose a strong directional bias on interactions with solvent, biomolecules, or nanoscale cargo. Nevertheless, the distinct differences in fibril density and network connectivity among the samples may still lead to substantial variation in gelation behavior, surface accessibility, and mechanical reinforcement.

CONCLUSIONS

In summary, quantitative analysis of electron microscopy images demonstrated that albumin, insulin, and lysozyme fibrils adopt distinct modes of supramolecular organization despite sharing a common amyloid-like structural framework.

The main findings are as follows: i) insulin exhibited the highest projected area fraction, skeleton length density, object density, endpoint density, and apparent junction/crossover density, indicating a compact and highly fragmented architecture dominated by numerous short rod-like elements; ii) lysozyme showed the highest median Feret length and aspect ratio, consistent with the formation of more elongated fibrillar objects and a stronger contribution of longitudinal growth; iii) albumin displayed an intermediate morphology characterized by relatively sparse, curvilinear fibrils and lower densities of discrete objects and endpoints; and iv) all three systems were globally weakly oriented, as reflected by broad angular distributions and low anisotropy indices, indicating predominantly isotropic rather than nematically ordered assemblies. From the perspective of amyloid physics, these results suggest that insulin occupies a fragmentation-dominated regime with a high density of fibril ends and potential interaction sites, whereas lysozyme is characterized by more extended anisometric objects that may favor the formation of continuous fibrillar pathways. Albumin represents an intermediate organizational state between these two regimes. Such differences are expected to influence surface accessibility, intermolecular association, network connectivity, diffusion within fibrillar matrices, and the mechanical behavior of amyloid-based materials. The combined use of projected area fraction, skeleton length density, endpoint density, apparent connectivity, local width, Feret length, aspect ratio, and orientation analysis provides a coherent framework for comparative fibril morphometry. These descriptors may support the rational selection of protein fibrils for hydrogels, biosensing, biomolecular immobilization, drug delivery, and nanocomposite development.

Acknowledgements

This work was supported by the Ministry of Education and Science of Ukraine (the project "Design of novel biocompatible nanocomposites and improvement of ultrasound-based diagnostic methods for medical applications" No. 0126U001036).

ORCID

Valeriya Trusova, https://orcid.org/0000-0002-7087-071X; **Uliana Malovytsia,** https://orcid.org/0000-0002-7677-0779
Olga Zhytniakivska, https://orcid.org/0000-0002-2068-5823; **Sergiy Bogatyrenko,** https://orcid.org/0000-0002-6044-6886;
Galyna Gorbenko, https://orcid.org/0000-0002-0954-5053

REFERENCES

[1] A. Taylor, and S. Radford, Curr. Opin. Struct. Biol. **98**, 103245 (2026). https://doi.org/10.1016/j.sbi.2026.103245
[2] A. Buell, Chem. Sci. **13**, 10177 (2022). https://doi.org/10.1039/d1sc06782f
[3] D. Li, and C. Liu, Structure **31**, 1335-1347 (2023). https://doi.org/10.1016/j.str.2023.08.006
[4] R. van der Kant, N. Louros, J. Schymkowitz, and F. Rousseau, Structure **30**, 1178 (2022). https://doi.org/10.1016/j.str.2022.05.002
[5] S. Basha, D. Mukunda, A. Pai, and K. Mahato, Int. J. Biol. Macromol. **311**, 143725 (2025). https://doi.org/10.1016/j.ijbiomac.2025.143725
[6] S. Gras, L. Waddington, and K. Goldie, Methods Mol. Biol. **752**, 197 (2011). https://doi.org/10.1007/978-1-60327-223-0_13
[7] R. Polon, C. Heard, O. Gonzales-Viera, M. Macías-Rioseco, A. Mete, K. Watson, L. Woods, and A. Armién, J. Vet. Diagn. Invest. **37**, 429-438 (2025). https://doi.org/10.1177/10406387251321415
[8] Y. Baek, and M. Lee, Biochem. Soc. Trans. **52**, 1631 (2024). https://doi.org/10.1042/BST20230854
[9] L. Morozova-Roche, J. Zurdo, A. Spencer, W. Noppe, V. Receveur, D. Archer, M. Joniau, and C. Dobson, J. Struct. Biol. **130**, 339 (2000). https://doi.org/10.1006/jsbi.2000.4264
[10] J. Schindelin, I. Arganda-Carreras, E. Frise, V. Kaynig, M. Longair, T. Pietzsch, S. Preibisch, *et al*, Nat. Methods, **9**, 676 (2012). https://doi.org/10.1038/nmeth.2019
[11] J. Adamcik, and R. Mezzenga, Angew. Chem. Int. Ed. Engl. **57**, 8370 (2018). https://doi.org/10.1002/anie.201713416
[12] T. Knowles, and R. Mezzenga, Adv. Mater. **28**, 6546 (2016). https://doi.org/10.1002/adma.201505961
[13] W. Xue, and S. Radford, Biophys. J. **105**, 2811 (2013). https://doi.org/10.1016/j.bpj.2013.10.034
[14] S. Hill, J. Robinson, G. Matthews, and M. Muschol, Biophys. J. **96**, 3781 (2009). https://doi.org/10.1016/j.bpj.2009.01.044

КІЛЬКІСНИЙ АНАЛІЗ МОРФОЛОГІЇ АМІЛОЇДНИХ ФІБРИЛ МЕТОДОМ ТРАНСМІСІЙНОЇ ЕЛЕКТРОННОЇ МІКРОСКОПІЇ

Валерія Трусова[1], Уляна Маловиця[1], Ольга Житняківська[1], Катерина Чкуаселі[1], Сергій Богатиренко[2], Галина Горбенко[1]

[1]Кафедра медичної фізики та біомедичних нанотехнологій, Харківський національний університет імені В.Н. Каразіна, м. Свободи 4, Харків, 61022, Україна

[2]Кафедра матеріалів реакторобудування та фізичних технологій, Харківський національний університет імені В.Н. Каразіна, м. Свободи 4, Харків, 61022, Україна

Амілоїдні фібрили дедалі частіше розглядають як універсальні білкові наноматеріали, функціональні властивості яких визначаються не лише молекулярною крос-β-архітектурою, а й особливостями їхньої надмолекулярної морфології. Метою цієї роботи було порівняння мезомасштабної організації фібрилярних агрегатів альбуміну, інсуліну та лізоциму із застосуванням кількісної трансмісійної електронної мікроскопії (ТЕМ). Репрезентативні ТЕМ-зображення було проаналізовано за допомогою стандартизованого алгоритму цифрової обробки, що включав сегментацію, скелетизацію, аналіз орієнтації та морфометрію зв'язних компонентів. Визначено проєкційну частку площі, зайняту фібрилами й агрегатами, щільність довжини скелетизованих структур, уявну щільність вузлів/перетинів і кінцевих точок, локальну ширину, щільність об'єктів, довжину Фере, співвідношення сторін та анізотропію орієнтації. Для інсуліну було встановлено найвищі значення проєкційної частки площі, щільності довжини скелетизованих структур, щільності об'єктів, кінцевих точок і уявних вузлів/перетинів, що свідчить про формування компактної, високофрагментованої архітектури з переважанням

численних коротких паличкоподібних елементів. Натомість, фібрили лізоциму характеризувалися найбільшими медіанними значеннями довжини Фере та співвідношення сторін, що узгоджується з більш вираженим поздовжнім ростом і формуванням анізометричних структур. Для альбуміну було виявлено проміжний тип морфології, який характеризується порівняно розрідженими криволінійними фібрилами та нижчою щільністю дискретних об'єктів і кінцевих точок. Для всіх трьох систем спостерігалися широкі розподіли орієнтацій і низькі індекси анізотропії, що вказує на переважно ізотропну, а не глобально впорядковану організацію. Отримані результати свідчать, що досліджені білкові системи реалізують різні режими амілоїдної самоорганізації, від архітектур із домінуванням фрагментації до більш протяжних фібрилярних мереж. Запропонований кількісний підхід створює основу для встановлення взаємозв'язку між морфологією амілоїдів, доступністю поверхні, зв'язністю, механічними властивостями та проєктуванням фібрилярних гідрогелів, біосенсорів, систем доставки лікарських засобів і нанокомпозитів.

Ключові слова: *амілоїдні фібрили; трансмісійна електронна мікроскопія; кількісний аналіз зображень; морфологія фібрил; надмолекулярна організація; скелетизація; анізотропія орієнтації; білкові наноматеріали*